9624 *J. Phys. Chem. A* **2009,** *113,* 9624–9632

Perchloromethyl Mercaptan, CCl_3SCl, Excited with Synchrotron Radiation in the Proximity of the Sulfur and Chlorine 2p Edges: Dissociative Photoionization of Highly Halogenated Species

Emiliano Cortés,[†] Carlos O. Della Védova,*[,†,‡] Mariana Geronés,[†] Rosana M. Romano,[†] and Mauricio F. Erben*[,†]

CEQUINOR (UNLP - CONICET, CCT La Plata), Departamento de Química, Facultad de Ciencias Exactas, Universidad Nacional de La Plata, CC 962, La Plata (CP 1900), República Argentina, and Laboratorio de Servicios a la Industria y al Sistema Científico (LaSeISiC) (UNLP-CIC-CONICET), Camino Centenario e/505 y 508, (1903) Gonnet, República Argentina

Received: May 14, 2009

We have investigated the dissociative photoionization of shallow-core excited CCl_3SCl by using multicoincidence time-of-flight mass spectrometry and synchrotron radiation in the S 2p and Cl 2p edges. The relative abundances of the ionic fragments and their kinetic energy release values were obtained from both PEPICO (photoelectron photoion coincidence) and PEPIPICO (photoelectron photoion photoion coincidence) spectra. The dynamic of the ionic fragmentation of S and Cl 2p excited CCl_3SCl has been studied and compared with those of CCl_4. Features determined in the present study seem to be relevant aspects for explaining the dissociation of highly chlorinated species under the action of VUV irradiation. The fragmentation pattern shows that chlorine ion (Cl^+) is prominently formed upon both S and Cl 2p excitations.

Introduction

Photoionization techniques are well-established methods for studying the spectroscopy of isolated molecules and the dynamic of the ionic species formed under the action of vacuum ultraviolet irradiation. In particular, halogenated alkanes have attracted attention as archetypal compounds for studies related to site-specific fragmentation of a core excited molecule.[1] For instance, as suggested by Schmelz et al.,[2] H_2CBrCl preferentially dissociates along the C−Br or C−Cl bonds after Br 3d or Cl 2p ionization, respectively. The strong site selectivity in the fragmentation was further probed by Miron et al. using energy-selected Auger electron photoion coincidence.[3] These kinds of studies are of interest from both fundamental and applied points of view. For example, it is well known that in the stratosphere, chlorocontaining haloalkanes are dissociated by UV or VUV irradiation to produce Cl atoms, which can then lead to the catalytic decomposition of ozone. Lin et al.[4] photodissociated CH_3Cl at 157.6 nm, and the reaction products were probed by VUV photoionization by synchrotron radiation. However, studies on this type of species using more energetic photons are less common; relevant examples that are mainly devoted to chloro-methyl derivatives[5] are CCl_4,[6] $CHCl_3$,[7−9] CH_2Cl_2,[10] and CH_3Cl.[11]

Our research group has quite recently started a systematic study of the electronic properties of shallow- and inner-core level in carbonylsulfenyl-chloride compounds with general formula XC(O)SCl. Therefore, FC(O)SCl,[12,13] ClC(O)SCl,[14] and $CH_3OC(O)SCl$[15] species have been studied by the use of synchrotron radiation in the 100−1000 eV range, and their ionic fragmentation after electronic decay has been analyzed. Most recently, we have succeeded in analyzing the electronic structure and ionic dissociation induced by photon absorption in the outermost valence region of chlorine- and sulfur-containing species. This study used a combined experimental approach that includes HeI photoelectron spectroscopy and photoionization under the action of synchrotron radiation in the 10−22.5 eV region.[16−18] Other studies on divalent sulfur compounds were devoted to the ionic dissociation of S 2p excited thioacetic acid [$CH_3C(O)SH$][19] and more recently methyl thiocyanate (CH_3SCN).[20]

Here we report a study of the photon impact excitation and dissociation dynamics on the highly chlorinated species CCl_3SCl, exited at shallow-core levels by using synchrotron radiation.

Trichloromethane sulfenyl chloride (perchloromethyl mercaptan, PCMM), CCl_3SCl, was first prepared in 1873 by Rathke,[21] following for its preparation the reaction between CS_2 and Cl_2 in the presence of a catalytic quantity of iodine at a temperature below 30 °C, a method that is still used commercially. PCMM received great industrial attention since Kittleson[22] discovered the 1,2,3,6-tetrahidro-*N*-(triclorometiltio)fthalimida derivative (commercially known as Captan), a compound that has extensive application in agriculture, being utilized primarily as a general fungicide for the treatment of a wide variety of foliar, soil, and seedborne diseases. Indeed, it was reported that virtually all derivatives of PCMM that have been prepared are potential pesticides.[23,24] Outstanding reviews covering the chemistry of PCMM can be found in the chemical literature.[25,26]

Of close interest for the present work, the infrared and Raman spectra of PCMM were carefully investigated, and the assignment of bands is consistent with the presence of a molecule belonging to the C_1 point group symmetry in the liquid phase.[27] Quantum chemical calculations suggest that the trans C_s conformer is present in the vapor (one chlorine atom in the $-CCl_3$ group and the chlorine atom in the S−Cl group in a mutual trans orientation).[28] The HeI photoelectron spectrum of

---

* To whom correspondence should be addressed. E-mail: carlosdv@quimica.unlp.edu.ar (C.O.D.V.); erben@quimica.unlp.edu.ar (M.F.E.).

[†] Universidad Nacional de La Plata.

[‡] Laboratorio de Servicios a la Industria y al Sistema Científico.

10.1021/jp904515u CCC: $40.75

CCl_3SCl was recorded very recently by Ge et al.,[28] and a molecular orbital assignment for the outer valence electron distribution was proposed.

In this work, we have recorded the total ion yield (TIY) spectra of PCMM at the S 2p and Cl 2p regions by using synchrotron radiation as a photon source. Multicoincidence PEPICO and PEPIPICO mass spectrometry has been applied to analyze the dissociation dynamics of the ionic fragmentation that follows the photon−molecule interaction.

Experimental Section

Synchrotron radiation was used at the Laboratório Nacional de Luz Síncrotron (LNLS), Campinas, São Paulo, Brazil. Linearly polarized light monochromatized by a toroidal grating monochromator (available at the TGM beamline in the range 12−300 eV)[29] intersects the effusive gaseous sample inside a high vacuum chamber, with base pressure in the range of 10^{-8} mbar. During the experiments, the pressure was maintained below 5×10^{-6} mbar. The resolution power is better than 400 in the TGM beamline at the LNLS. The energy calibration was established by means of the S 2p $\rightarrow 6a_{1g}$ and S 2p $\rightarrow 2t_{2g}$ absorption resonances in SF_6.[30] The intensity of the emergent beam was recorded with a light-sensitive diode. The ions produced by the interaction of the gaseous sample with the light beam were detected using a time-of-flight (TOF) mass spectrometer of the Wiley−McLaren type for both PEPICO and PEPIPICO measurements.[31,32] This instrument was constructed at the Institute of Physics, Brasilia University, Brasilia, Brazil.[33] The axis of the TOF spectrometer was perpendicular to the photon beam and parallel to the plane of the storage ring. Electrons were accelerated to a multichannel plate (MCP) and recorded without energy analysis. This event starts the flight time determination process of the corresponding ion, which is consequently accelerated to another MCP. The characteristics and performance of this electron−ion coincidence TOF spectrometer have recently been reported.[34] To achieve a good mass resolution in PEPICO and specially PEPIPICO spectra, long acquisition times were spent to gather useful coincidence statistics.

We calculated the average kinetic energy release (KER) values of the fragments from the coincidence spectra by assuming an isotropic distribution of the fragments and assuming that they are perfectly space-focused and that the electric field applied in the extraction region is uniform.[35] Under these conditions, the KER[36,37] in the fragmentation process can be determined from the peak width following the method suggested by Pilling et al.[38] Deviations from ideal conditions always increase the peak width, and thus the values calculated are upper bounds. Santos et al.[39] have measured the argon mass spectrum under very similar experimental conditions, and a peak width value of 0.05 eV was achieved for the Ar^+ ion. Because the broadening in argon can only be the result of thermal energy and instrumental broadening, this value represents a good estimation for the instrumental resolution.

The sample of CCl_3SCl was obtained from commercial sources (Aldrich, estimated purity better than 97%). The liquid sample was purified by repeated trap-to-trap vacuum distillation. The purity of the compound was checked by IR spectroscopy.[27]

Results and Discussion

The CCl_3SCl molecule in the ground electronic state belongs to the C_s symmetry point group. Then, for further reference, all canonical molecular orbitals of type a′ are σ orbitals lying in the molecular plane, whereas those of type a″ are π orbitals.

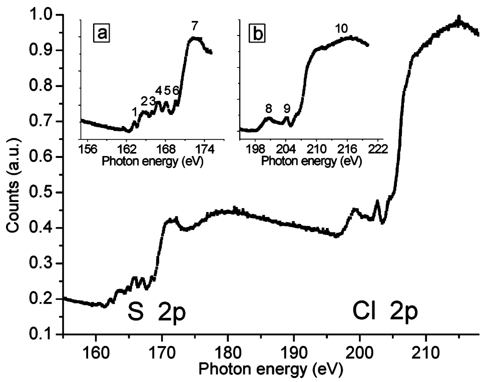

Figure 1. Total ion yield spectrum for CCl_3SCl in the S 2p and Cl 2p regions. Inset (a): Transitions below S 2p threshold, bands centered at: 163.2 eV (1), 164.5 eV (2), 165.8 eV (3), 166.9 eV (4), 168.1 eV (5), 169.5 eV (6), and 172.3 eV (7). Inset (b): Transitions below Cl 2p threshold, bands centered at: 200.7 eV (8), 204.0 eV (9), 215.7 eV (10).

The outermost electronic distribution reveals that the HOMO, having a″ symmetry, can be visualized as an orbital nominally localized on the sulfur atom occupied by lone-pair electrons. Its vertical ionization potential value is 9.61 eV.[28] The following bands in the PES spectrum were assigned to a series of lone-pair electrons in orbitals with a′ and a″ symmetry nominally localized on the various chlorine atoms in the molecule. The bonding orbital of the S−Cl σ bond (σ_{S-Cl}) appears at higher energies, having a ionization energy of 14.10 eV. This description of the outermost occupied orbitals for PCMM is consistent with the electronic structure reported for molecules containing the trichloromethane sulfenyl moiety, CCl_3SX, X = SCN,[40] $OC(O)CH_3$, and $OC(O)CF_3$.[28]

Total Ion Yield Spectra. We have investigated the shallow-core electron distribution of gaseous PCMM by measuring the TIY spectra in the VUV region (from 100 to 250 eV) using tunable synchrotron radiation as an adequate photon source. The TIY spectra were obtained by recording the count rates of the total ions while the photon energy was scanned. At high photon energies corresponding to shallow-core electronic levels, the quantum yield for molecular ionization was quite likely tending to unity. Consequently, the detection of the parent and fragment ions as a function of the incident photon energy is a powerful method to be used as a complement to the absorption spectroscopy.[41]

The TIY spectrum of CCl_3SCl, measured near the S 2p and Cl 2p edges is shown in Figure 1. Below the S 2p threshold, the spectrum is dominated by a group of well-defined signals centered at 163.2, 164.5 (broad), 165.8, 166.9, 168.1, and 169.5 eV (Figure 1a). These resonant transitions should correspond to dipole-allowed transitions that involve excitations of an electron with marked 2p character to an antibonding molecular orbital. According to the angular momentum selection rule ($\Delta L \pm 1$), the final state should mainly have either d or s character.[42] Therefore, the well-resolved structures observed in the TIY spectra in the S 2p region can be interpreted to be originated by electronic transitions involving the spin−orbit split of the 2p sulfur excited species ($2p_{1/2}$ and $2p_{3/2}$ levels) mainly to the unoccupied σ^* antibonding orbitals. Quantum chemical calculations at the MP2/6-311+G(3df) level of approximation for neutral CCl_3SCl in its ground state compute that the LUMO is clearly a σ^*_{S-Cl} (a′) orbital with antibonding character. Three antibonding orbitals with similar energies ascribed as σ^*_{C-Cl} localized in the CCl_3− group and σ^*_{C-S} (a′) complete the

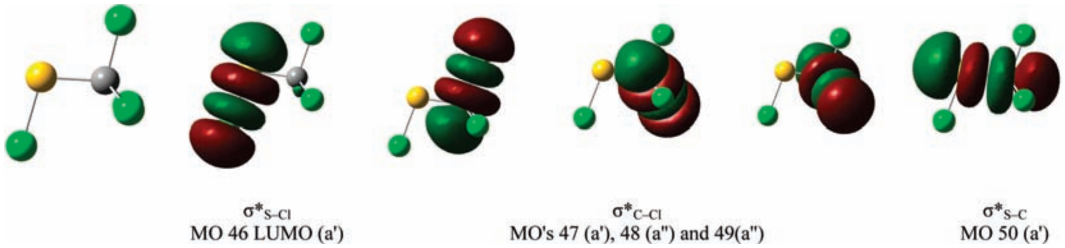

Figure 2. Optimized molecular structure and characters of the lower-energy unoccupied molecular orbitals for CCl_3SCl calculated at the MP2/6-311++G(3df) level of approximation.

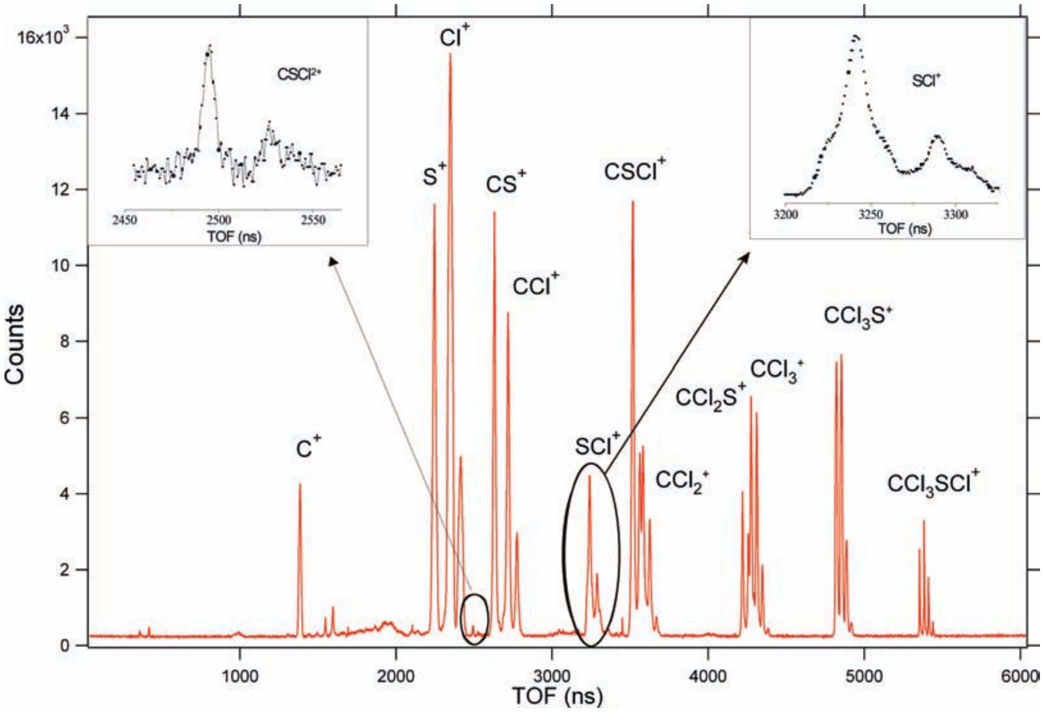

Figure 3. PEPICO spectrum at 166.9 eV with ion assignment for CCl_3SCl. The insets show an enlargement of the TOF regions for the $CSCl^{2+}$ (left) and SCl^+ (right) ions, respectively.

antibonding molecular orbital representation expected for PCMM. (See Figure 2.)

Taking into account the spin–orbit splitting of the S 2p term reported for H_2S (1.201 eV),[43] the first transitions observed in the TIY spectra at 163.2 and 164.5 eV were tentatively assigned to S 2p → σ^*_{S-Cl}. It should be noted, however, that the expected intensity ratio of 2:1 is not observed, denoting the presence of overlapping transitions. This hypothesis is reinforced by the fact that the 164.5 eV signal is broad and poorly resolved. It is probably because excitations to the σ^*_{C-Cl} vacant orbitals overlap with the S $2p_{1/2}$ → σ^*_{S-Cl} resonance. It is quite difficult at this point to assign with confidence the following peaks because transitions to the three σ^*_{C-Cl} orbitals should have quite similar but nonequal energies. The intense resonance at 166.9 eV is tentatively assigned to the S 2p → σ^*_{C-Cl} transition. On the basis of quantum chemical calculation results, the well-resolved 168.1 and 169.5 eV resonances are tentatively assigned to S 2p → σ^*_{C-S} transitions.

In Figure 1a, note the broad feature appearing near the ionization edge. This could be related to autoionization or shakeup processes, usually present in molecules possessing electronegative atoms. The occurrence of this feature precludes the estimation of the S 2p ionization potentials from the TIY spectrum.

The TIY spectra of PCMM obtained in the Cl 2p region exhibit a sharp edge at ca. 208 eV (see Figure 1). The 2p Cl binding energies in CCl_4 are 207.09 and 208.65 eV, as reported by Fournier et al.[44] As is apparent in Figure 1b, the distinction of Cl 2p transitions in the TIY spectrum for nonequivalent chlorine atoms in CCl_3SCl is not feasible at the accessible resolution of our measurements. Two broad and weak resonances are observed below the ionization edge at 200.7 and 204.0 eV, which are assigned to unresolved Cl 2p → σ^*_{C-Cl} transitions. Similar features, assigned to Cl $(2p^{-1})$→ σ* transitions, appear in the ion yield spectra of CH_3Cl.[11]

PEPICO Spectra. We have recorded PEPICO spectra by setting the photon energy at the whole resonant values observed in the TIY spectrum. To identify the role of the resonant processes in the fragmentation, we also measured the spectra at photon energy values below (typically 10 eV) and above (typically 50 eV) the estimated ionization.

The TOF spectrum of PCMM taken at 166.9 eV (at the S 2p → σ^*_{C-Cl} resonance energy) is shown in Figure 3 together with the ion assignment. The excellent mass resolution and signal-to-noise ratio achieved allows the distinction of naturally occurring isotopomer fragments because of the presence of ^{35}Cl and ^{37}Cl isotopes in the title molecule. This splitting assists the assignment of the ion fragments appearing in the coincidence spectra. The PEPICO spectra taken at representative photon energies near the S 2p and Cl 2p edges of CCl_3SCl are shown in Figures 4 and 5, respectively.

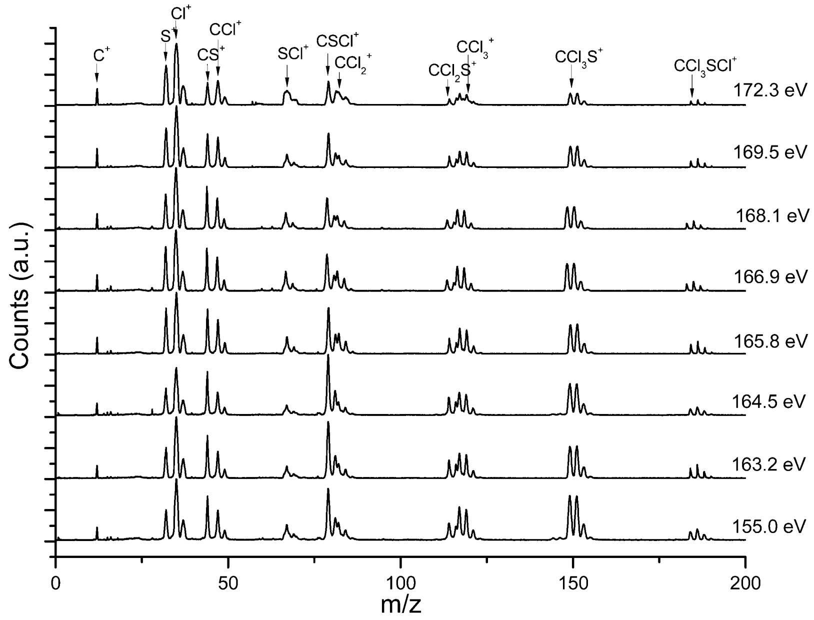

Figure 4. PEPICO spectra of CCl_3SCl at selected energies near the S 2p edge.

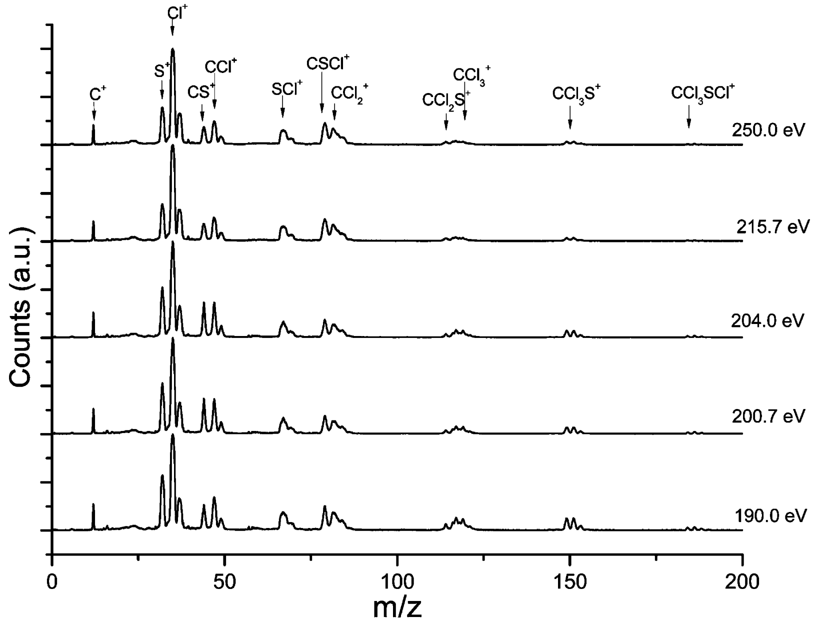

Figure 5. PEPICO spectra of CCl_3SCl at selected energies near the Cl 2p edge.

The molecular ion is clearly observed with the natural occurring isotopomeric and intensity ratio through the whole S 2p region. The most intense peaks observed in the PEPICO spectra over the whole range of energy studied corresponds to the Cl^+ ion, accounting for ca. 22−31% at the S 2p region, with a notorious enhancement at the Cl 2p region, reaching values of ca. 38−44%. The whole series of CCl_x^+ and CCl_xS^+ ions ($x = 1$, 2, and 3) is observed as an intense signal in the PEPICO spectra, the ions with $x = 1$ and 3; that is, CCl^+ and CCl_3^+ and $ClCS^+$ and Cl_3CS^+ are clearly more intense than CCl_2^+ and Cl_2CS^+. In the 166.9 eV spectrum, the CS^+ and SCl^+ diatomic cations are also present with an intensity of 7.4 and 6.4%, respectively. Finally, the C^+ and S^+ atomic fragments are present even at the lowest photon energy used in this work, accounting for 2.9 and 10.2% of the signal observed in the PEPICO spectrum taken at 166.9 eV. Therefore, the occurrence of processes leading to the atomization of PCMM can be anticipated. The branching ratios determined from the PEPICO spectra of CCl_3SCl at photon energies around the S 2p and Cl 2p edges are shown in Table 1.

From the PEPICO peak shape, the KER values have been determined for each ion. In Table 1, the values obtained at selected photon energies are given. Nearly identical KER values were determined at 155 (below the S 2p edge) and 166.9 eV (in resonance). These values are relatively low, with molecular and atomic fragment ions displaying KER lower than 1 eV and in the 2 to 3 eV range, respectively. A broadening in their peak widths is clearly observed above the S 2p edge (172.3 eV) and in the Cl 2p region, where all of the ions show higher KER values. This effect becomes apparent in the PEPICO spectra shown in Figure 5. It is well known that the decay of core-shell-excited species normally leads to the formation of doubly charged parent ions in several excited states, which could then dissociate releasing much of their internal energy as kinetic energy of the fragment ions.[35]

TABLE 1: Branching Ratios (%) and Kinetic Energy Release Values (eV) for Fragment Ions Extracted from PEPICO Spectra Taken at Photon Energies around the S and Cl 2p Edges for CCl_3SCl[a,b]

	S 2p								Cl 2p				
ion	155.0	163.2	164.5	165.8	166.9	168.1	169.5	172.3	190.0	200.7	204.4	215.7	250.0
C^+	2.2/*2.2*	2.3	2.7	2.7	2.9/*2.5*	3.0	3.3	3.4/*3.7*	4.2	4.5/*3.9*	4.4	4.0/*4.7*	3.9
S^+	7.2/*2.4*	7.8	7.3	10.2	10.2/*2.3*	9.7	11.6	13.2/*4.2*	15.1	14.7/*4.3*	14.6	12.0/*5.0*	12.0
Cl^+	22.1/*3.5*	23.9	19.8	23.6	23.9/*3.9*	26.3	28.1	30.8/*4.7*	38.3	40.6/*4.8*	40.4	44.0/*5.2*	43.3
CS^+	7.1/*0.80*	7.9	7.9	7.9	7.4/*0.77*	8.4	7.7	5.5/*1.5*	5.4	7.5/*1.3*	7.4	5.2/*2.9*	5.2
CCl^+	7.5/*0.92*	8.1	8.1	9.3	9.3/*0.96*	9.7	9.9	9.7/*2.1*	10.5	11.0/*1.8*	11.1	11.5/2.9	9.1
SCl^+	5.2/[c]	4.7	4.8	5.5	6.4/[c]	6.1	5.5	9.5/[c]	8.4	7.1	7.2	7.8	7.7
$CSCl^+$	11.4/*0.51*	13.6	14.6	10.8	9.2/*0.51*	9.0	9.6	7.1/*0.69*	6.1	5.4/*0.95*	5.3	8.0/*1.6*	7.9
$CCl_2{}^+$	6.3/*0.48*	5.5	6.2	6.3	7.0/*0.45*	5.9	5.3	7.4/[d]	1.5	1.6/[d]	1.8	1.8/[d]	5.7
$CSCl_2{}^+$	4.5/*0.18*	4.5	5.2	3.5	3.3/*0.14*	3.1	2.9	2.0/*0.16*	1.6	1.3/*0.28*	1.2	1.4/*0.74*	1.3
$CCl_3{}^+$	9.4/*0.21*	7.9	7.8	7.7	8.0/*0.18*	7.3	5.8	5.5/*0.19*	4.5	3.3/*0.69*	3.4	1.8/[d]	2.0
$CSCl_3{}^+$	14.0/*0.19*	11.3	12.4	10.2	9.8/*0.18*	9.0	8.5	4.7/*0.18*	3.6	2.5/*0.20*	2.5	1.6/*0.48*	1.5
CCl_3SCl^+	3.0/*0.053*	2.5	3.3	2.3	2.6/*0.013*	2.5	1.8	1.2/*0.026*	0.8	0.7/*0.069*	0.6	0.5/[e]	0.4

[a] Peaks for the corresponding naturally occurring isotopomer were observed and added together. [b] Kinetic energy release values determined at selected energies are given in italics. [c] Doble KER distribution is observed (see the text). [d] Overlapping of peaks is observed. [e] Too low intensity to be measured.

To the best of our knowledge, the double-ionization potential of CCl_3SCl has not been reported. For the related species CCl_4, the lower double-ionization energy to singlet states is 29.1 ± 0.1 eV, and calculations predict that most of the dissociative channels are opened at energies above 43.85 eV.[45] Consequently, 155.0 eV photons should be adequate to open most of the possible ionization channels connected to the direct single and double ejections of valence-shell electrons. As observed in the TIY spectra, this energy is not yet enough to ionize the S 2p shallow-core electrons. Therefore, the coincidence spectrum taken at 155.0 eV photon energy should provide a good comparison with respect to the ionic fragmentation pattern associated with core excitations or ionizations.

The single-charged molecular ion is observed in the whole range of photon energies studied. Nevertheless, a clear diminution of the peak intensity for the CCl_3SCl^+ ion is observed when resonant energies are reached, with typical abundance values of ~2% at the S 2p transitions. When Cl 2p electrons are ionized, further diminution in the signal intensity becomes apparent, and a nearly negligible contribution of M^+ is observed in the PEPICO spectra above 200.7 eV, as shown in Figure 5. As expected, the KER values determined for this ion are close to the "thermal" value of 0.05 eV.[39]

At this point, it is interesting to compare the behaviors observed for PCMM and carbon tetrachloride, CCl_4. The latter species has been extensively studied, and the similarity with the title species resides in the fact that PCMM can be formally thought of as a CCl_3X derivative, with X = SCl. Indeed, both compounds have four chlorine atoms in their molecular formula, and sulfur and chlorine have quite similar electronegativity values (2.44 and 2.83, respectively, on the Allred and Rochow scales). The instability of tetrahalide ions such as $CCl_4{}^+$ has been studied by threshold photoelectron−photoion coincidence (TPEPICO) spectroscopy and synchrotron radiation in the range of 14−23 eV. The $^2T_2$ and $^2A_1$ states of $CCl_4{}^+$ fragment exclusively to $CCl_2{}^+$ and CCl^+, respectively, corresponding to nonstatistical routes.[46] Also, Eland and coworkers observed orientation and alignment of photoelectrons relative to $CCl_3{}^+$ fragments from photoionization to the low-lying state of $CCl_4{}^+$ by using the velocity imaging photoionization coincidence technique.[47] Kime et al.[48] have suggested that $CCl_4{}^+$ is thermodynamically unstable and dissociates exothermically into $CCl_3{}^+$ + Cl upon electron impact. Kischlat and Morgner,[49] using electron−ion coincidence spectra, have showed that $CCl_4{}^+$ primarily dissociates into $CCl_2{}^+$.

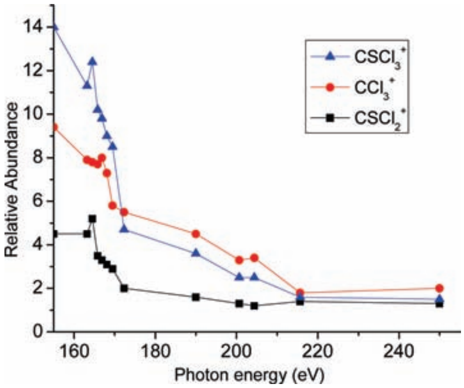

Figure 6. Partial ion yield (PIY) for selected series of ions following photon excitation of CCl_3SCl as a function of photon energy.

On the basis of these considerations, the partial ion yields for CCl_3S^+, CCl_2S^+, and $CCl_3{}^+$ ions for PCMM are depicted in Figure 6. A similar ion dependence on the photon energy is observed because the ions decrease their signal intensity when the photon energy is increased. This effect is especially noticeable for CCl_3S^+, with intensities of 14.0 and 4.7% at 155.0 and 172.3 eV, respectively. The relatively low KER values observed for these ions, ca. 0.20 eV, suggest the extrusion of neutral fragments (one or two chlorine atoms and SCl group) from single-charged CCl_3SCl^+ to produce CCl_3S^+, CCl_2S^+, and $CCl_3{}^+$, respectively (eqs 1−3)

$$CCl_3SCl^+ \rightarrow CCl_3S^+ + Cl \tag{1}$$

$$CCl_3SCl^+ \rightarrow CCl_2S^+ + 2\,Cl \tag{2}$$

$$CCl_3SCl^+ \rightarrow CCl_3^+ + SCl \tag{3}$$

It should be noted that the detection of such a heavy fragment in the PEPICO spectra of PCMM implies that all of them should be produced from a single-charged molecular ion. Moreover, the KER values determined for these ions are consistent with the maximum KER values determined for $CCl_4{}^+$.[50] When PCMM is irradiated with 155.0 eV photons in the valence continuum region of the spectrum, reactions 1−3 yield about 28% of observed ions in the PEPICO spectrum.

Processes that yield charged chlorine atoms (Cl^+) are evident from the intense signal at *m*/*z* = 35 amu/*q*. The production of

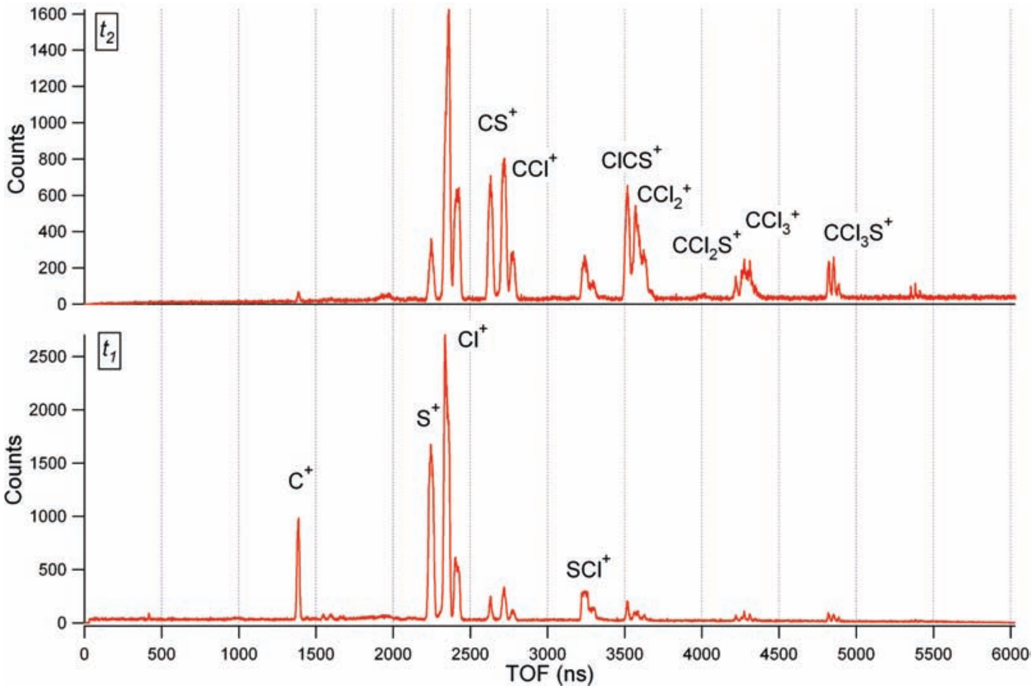

Figure 7. t_1 and t_2 projections of the PEPIPICO spectrum of CCl_3SCl recorded at 166.9 eV.

Cl^+ represents 23% of ions found at energies around the S 2p edge, reaching as much as 44% at 215.7 eV, in the Cl 2p region. An unambiguous description of these processes is not possible at this point because several dissociation channels could generate this ion, obscuring the interpretation. It should be noted, however, that the high KER value determined for the Cl^+ ion denotes the ejection of energetic ions.

The rupture of the sulfur−carbon bond in PCMM to yield the SCl^+ ion can also be inferred from the PEPICO spectra. From the peak shape, a clear double-KER distribution can be recognized for the signal at TOF, between 3200 and 3330 ns, as shown in the inset of Figure 3. This behavior could be rationalized in the case that this ion is generated from both single- and double-charged molecular ions according to eqs 4 and 5

$$CCl_3SCl^+ \rightarrow CCl_3 + SCl^+ \tag{4}$$

$$CCl_3SCl^{2+} \rightarrow CCl_x^+ + SCl^+ + (3-x)Cl \quad (x = 2 \text{ to } 3) \tag{5}$$

Ions originated in the process given by eq 4 should have a narrower KER distribution than those arising from eq 5. When the photon energy is increased, the second dissociation channel is enhanced, and a broad peak is observed for this ion (SCl^+).

As mentioned before, a common feature of the single-charged ions is the peak broadening observed upon moving from 155.0 eV in the inner-valence through the S 2p to Cl 2p regions, denoting the importance of Auger-induced double-ionization and fragmentation processes. Therefore, multicoincidence spectra allowing for the detection of at least two ions are required to analyze the dynamic of fragmentation of S and Cl 2p excited CCl_3SCl.

PEPIPICO Spectra. Two-dimensional PEPIPICO spectra for the correlation between one electron and two positive ions were recorded at each of the resonant energy values in the S 2p and Cl 2p regions. We obtained projections of PEPIPICO spectra of CCl_3SCl on the t_1 and t_2 axes by integrating the signal intensities over the corresponding time domains. These projections for the spectrum recorded at 166.9 eV are depicted in Figure 7. The Cl^+ ion signal dominates both the t_1 and t_2 domains, meaning that this ion could be either the lighter or the second-lighter ion in dissociative events. For instance, it becomes apparent that Cl^+ is the heaviest ion detected with this technique for dissociations of PCMM involving the concomitant production of C^+ or S^+ (lighter ions than Cl^+), whereas events for which Cl^+ is the lightest ion could imply coincidences with CCl_x^+ ($x = 1$ to 3), SCl^+, or CCl_xS^+ ($x = 0$ to 3) ions. The series of CCl_x^+ ($x = 1$ to 3) and CCl_xS^+ ($x = 0$ to 3) ions appear as intense signals, mainly in the t_2 domain. As expected for PCMM, C^+ acts exclusively as the lightest ion, being observed only in the t_1 domain. S^+ is mainly produced in dissociation processes where it is also the first ion arriving to the detector. The medium intensity signal observed for S^+ in the t_2 domain must be associated with processes producing entirely C^+/S^+ coincidence. The identification of CS^+ mostly appearing in the t_2 domain implies that Cl^+ is produced together as the lightest ion. The heaviest fragment observed in the t_2 domain is the M-35 ion. Finally, very weak signals observed for CCl_3^+ and CCl_3S^+ ions in the t_1 domain as well as a weak feature at 1485 ns (C^+) in t_2 are associated with false coincidences.

It is well known that core excitation and core ionization lead to resonant and normal Auger processes, which are highly effective electronic decay mechanisms in promoting the dissociation of molecules. The analysis of the PEPIPICO spectra is useful for identifying two-, three-,[31] and four-body dissociation mechanisms, which especially follow Auger decay mechanisms.[51,52]

At this point, to have more information from related systems, it is interesting to stress some of the prominent features already reported for the species CCl_4. The CCl_4^{2+} ion has been studied using charge-transfer spectroscopy and X-ray-induced Auger-electron spectroscopy. The results were interpreted in terms of bound or flat potential curves in the doubly ionized states, which

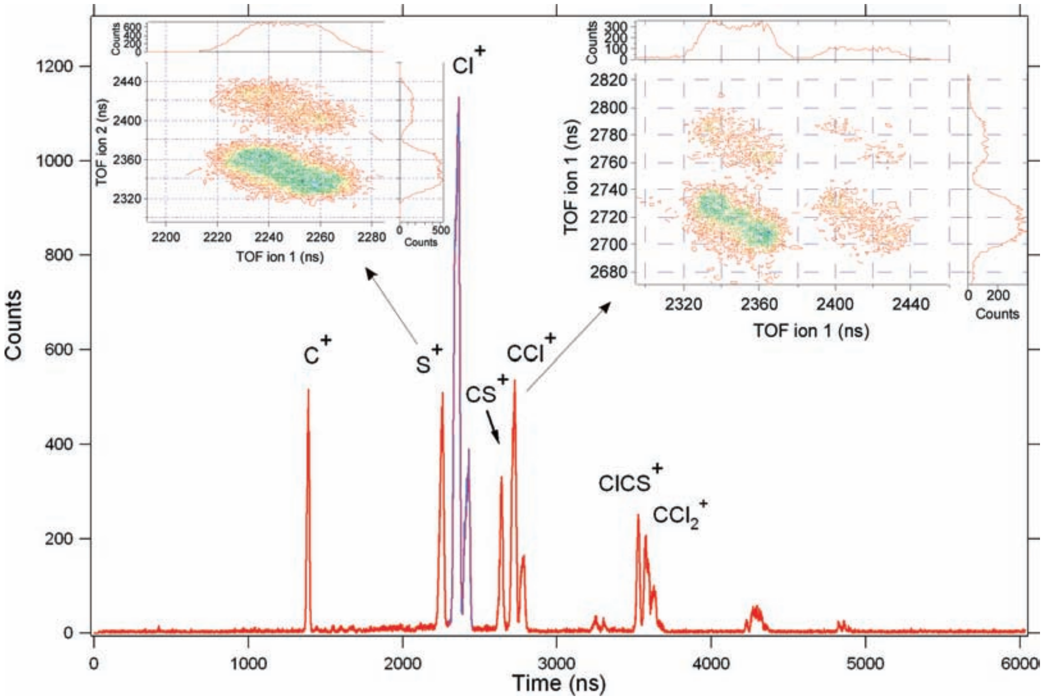

Figure 8. Projection spectrum over the Cl^+ arriving time recorded at 166.9 eV for CCl_3SCl. Contour plots for the double-coincidence islands between S^+/Cl^+ (left) and Cl^+/CCl^+ (right) ions derived from the PEPIPICO spectrum of CCl_3SCl are shown in the insets.

are presumably either stable or quasistable.[44] Conversely, the formation and decay of dication states of CCl_4 following the 2p Cl ionization has been studied in an electron impact experiment by Auger electron−ion coincidence measurements.[50] No evidence of either bound stable or metastable CCl_4^{2+} states has been observed, and the fragmentation pattern of the dications resulted in being strongly dependent on the state and geometry of the dication.[6,50] Moreover, the double-charged CCl_3^{2+} ion is observed around both the Cl 2p and Cl 1s edges of CCl_4 and presents a very narrow structure.[50] This could be explained by taking into consideration the fact that the doubly charged molecular ion dissociates, in this case, into CCl_3^{2+} and neutral chlorine atom. Further improvement in the mass resolution allows the observation of highly charged Cl^{2+}, CCl^{2+}, and CCl_2^{3+} ions for CCl_4 excited with synchrotron radiation around the Cl 2p and C 1s edges.[6] For PCMM, double-charged molecular ion CCl_3SCl^{2+} is unstable on the microsecond time scale and cannot be observed in our experiments. The $CSCl^{2+}$ dication is observed as a weak signal at $m/z = 39.5$ over the whole range of photon energies studied here. (See the inset in Figure 3.)

As previously discussed, the importance of the atomization processes in the dissociation mechanisms of CCl_3SCl could be anticipated. These processes may be originated by several multibody dissociation events that conduce to the same final pair of atomic ions, making ambiguous the analysis of these coincidences as appearing in the PEPIPICO spectra. Moreover, the TOF apparatus used in this work is unable to identify chlorine atoms arising from dissociation of CCl_3 and SCl groups in the molecule directly.

The importance of Cl^+ ion contribution to the double-coincidence spectra can be inferred from the projection spectrum shown in Figure 8 for times corresponding to ions arriving in the 2290−2455 ns range (including both $^{35}Cl^+$ and $^{37}Cl^+$ ions). The Cl^+/Cl^+ coincidence as well as coincidences between atomic and fragment ions are anticipated.

The double-coincidence branching ratio for double-ion processes calculated from PEPIPICO spectra at several photon energies is given in Table 2. The contribution of double coincidences involving the Cl^+ ion has been semiquantitatively determined. Therefore, as much as 75.7% of the double coincidences originated from PCMM have the Cl^+ ion as either the lightest (50.3%) or the second-lightest (25.4%) ion in the spectrum recorded at 155.0 eV. This contribution increases when the Cl 2p edge is reached, accounting for 80.2% at the 200.7 eV resonance. Among others, S^+/Cl^+, Cl^+/CS^+, Cl^+/CCl^+, and $Cl^+/ClCS^+$ are the most intense coincidences. For instance, the former accounts for ca. 30% of double ionizations observed at 200.7 and 204.0 eV in the Cl 2p region.

The contour plot of the double coincidences between the S^+/Cl^+ pair of ions is shown in the inset of Figure 8. As mentioned, this coincidence can be originated from several dissociation mechanisms involving the atomization of PCMM. Indeed, a nondefined shape is observed in PEPIPICO, indicating the contribution of several dissociation processes. A similar behavior is found for the C^+/Cl^+ double coincidence. Taking into consideration these facts, attention is paid to selected pairs of ions for which both good statistics and well-defined shapes are observed. The experimental slopes for coincidence islands were determined at both resonance and off-resonance photon energies in the S 2p and Cl 2p regions, and no significant changes in the dissociation mechanism were observed. The following discussion will be referred to slopes determined from the PEPIPICO spectrum taken at 166.9 eV photon energy.

Fragmentation processes leading to the formation of CCl_3^+ and SCl^+ ions are observed as a low intensity island at both the S 2p and Cl 2p levels. The parallelogram-like shape of the island and the observed slope close to −1.0 can be explained by a two-body mechanism

$$CCl_3SCl^{2+} \rightarrow CCl_3^+ + SCl^+ \quad (KER = 3.6\ eV)$$

TABLE 2: Relative Intensities for Double-Coincidence Islands Derived from the PEPIPICO Spectra of CCl_3SCl As a Function of the Photon Energy[a]

		S 2p								Cl 2p				
ion 1	ion 2	155.0	163.2	164.5	165.8	166.9	168.1	169.5	172.3	190.0	200.7	204.0	215.7	250.0
C^+	S^+	1.8	2.1	2.1	3.3	3.2	2.9	3.8	3.4	4.4	4.4	4.3	2.7	2.7
C^+	Cl^+	6.0	6.7	6.2	7.5	7.5	8.0	8.1	6.6	9.6	10.8	10.6	9.0	8.6
C^+	SCl^+				0.2	0.1	0.1	0.1	0.3	0.3	0.2	0.2	0.2	0.2
S^+	Cl^+	19.4	19.3	18.4	20.7	20.8	21.6	22.3	18.6	26.5	29.2	29.0	21.5	20.7
S^+	CCl^+	6.6	7.6	10.0	9.6	8.5	7.7	9.3	8.8	9.8	8.7	8.8	7.6	6.2
S^+	CCl_2^+	2.1	2.4	2.2	3.3	3.0	1.9	2.6	4.3	0.3	0.2	0.2	0.3	2.1
S^+	CCl_3^+	0.6	0.7	0.3	1.0	0.9	0.6	0.6	2.4	1.8	1.1	1.1	0.5	0.4
Cl^+	CS^+	14.8	15.5	14.9	13.0	11.9	13.3	13.2	8.2	10.4	11.1	10.8	11.7	11.5
Cl^+	CCl^+	12.9	12.4	14.9	12.7	13.8	14.6	12.8	12.2	16.4	16.3	16.4	16.3	12.8
Cl^+	SCl^+	1.2	1.0	0.9	1.2	1.7	1.8	1.3	2.2	2.4	2.2	2.2	2.2	2.0
Cl^+	$CSCl^+$	16.9	17.8	16.5	14.0	13.1	13.5	13.1	10.7	9.7	9.0	9.0	17.0	16.5
Cl^+	CCl_2^+	2.0	1.1	0.9	1.2	1.9	1.4	0.9	2.3	0.2	0.3	0.3	0.6	2.4
Cl^+	$CSCl_2^+$	1.6	2.0	1.4	1.3	1.2	1.1	1.0	1.1	0.8	0.9	0.8	2.6	2.2
Cl^+	CCl_3^+	0.2	0.2	0.1	0.1	0.2	0.2	0.1	0.3	0.3	0.2	0.2	0.3	0.4
Cl^+	$CSCl_3^+$	0.7	0.6	0.5	0.5	0.6	0.6	0.5	0.3	0.2	0.2	0.2	0.8	0.7
CCl^+	SCl^+	3.6	3.1	3.7	3.7	4.0	3.8	3.2	4.4	3.8	3.0	3.2	5.5	4.4
SCl^+	CCl_2^+	8.3	6.3	6.0	5.4	6.1	5.6	5.6	10.2	0.6	0.4	0.6	0.7	5.8
SCl^+	CCl_3^+	1.4	1.2	0.8	1.4	1.4	1.4	1.3	3.8	2.6	1.7	2.0	0.5	0.5

[a] Islands for the corresponding naturally occurring isotopomer were observed and added together.

It is worthy to be mentioned that the existence of a two-body mechanism to give CCl_3S^+ and Cl^+ ions can be discarded because a double coincidence involving these ions is not observed over the whole range of studied photon energies.

The coincidence between the SCl^+ and CCl_2^+ ions with a relative abundance of ca. 6% in the S 2p region with an experimental slope of −1.0 can be explained by a deferred charge separation mechanism[52]

$$CCl_3SCl^{2+} \rightarrow CCl_2SCl^{2+} + Cl \quad (KER = 3.8 eV)$$

$$CCl_2SCl^{2+} \rightarrow CCl_2^+ + SCl^+$$

Therefore, it is likely that the chlorine atom ejected in the first step comes from the CCl_3 group, whereas the CCl_2SCl^{2+} ion undergoes a second dissociation process to give the detected fragments. This dissociation mechanism could be responsible for the broad KER associated with the SCl^+ ion, reflected in the peak shape observed in the PEPICO spectra. (See eq 5 and Figure 3.)

For the S^+/CCl_2^+ pair of ions, a medium intensity coincidence with a branching ratio of 3.0% at 166.9 eV is observed with a −0.7 slope. In principle, several dissociation channels can be proposed to explain this coincidence. According to Simon et al.,[52] the following four-body secondary decay after a deferred charge separation mechanism is proposed

$$\begin{aligned} &CCl_3SCl^{2+} \rightarrow CCl_3S^{2+} + Cl \\ &CCl_3S^{2+} \rightarrow CCl_3^+ + S^+ \qquad (KER = 4.0\ eV) \\ &CCl_3^+ \rightarrow CCl_2^+ + Cl \end{aligned}$$

The calculated slope of $-0.70[-m_{CCl_2}/(m_{Cl} + m_{CCl_2})]$ is in perfect agreement with the value derived from the PEPIPICO spectra.

The contour plot for the Cl^+/CCl^+ double coincidence is shown in an inset in Figure 8. The experimental slope determined for this island is −0.81, which can be explained in terms of a secondary decay in the competition mechanism[52] involving the following dissociation steps

$$\begin{aligned} &CCl_3SCl^{2+} \rightarrow CCl_3^+ + SCl^+ \\ &CCl_3^+ \rightarrow CCl^+ + 2Cl \qquad (KER = 4.0\ eV) \\ &SCl^+ \rightarrow Cl^+ + S \end{aligned}$$

If the KER corresponding to the neutral ejections is neglected,[53] then the associated shape of the peak is a parallelogram with a slope equal to $-[m_{CCl}/(m_{CCl} + 2m_{Cl})]/[m_{Cl}/(m_{Cl} + m_S)] = -0.77$, which is in very good agreement with the experimental value. Other feasible four-body mechanisms, such as the deferred charge separation or the secondary decay after a deferred charge separation,[52] would be able to explain the coincidence between the Cl^+ and CCl^+ ions but would fail to explain the observed slope island with calculated values of −1.0 and −0.57, respectively.

Conclusions

A detailed study of the ionic fragmentation of the CCl_3SCl molecule in the gas phase following continuum valence and shallow-core (S 2p and Cl 2p) excitations has been performed using multicoincidence techniques based on time-of-flight mass spectrometry and synchrotron radiation as the photon source.

Dissociation mechanisms have been proposed to explain the ionic fragmentation decay for single- and double-charged core-excited PCMM. Cl^+ ions are present in the products of several of these dissociation channels. Therefore, it is observed that the relative intensity of molecular ions containing chlorine (such as CCl_x^+ and CCl_xS^+, $x = 1$ to 3) decreases with increasing photon energy, whereas the relative intensity of the Cl^+ ion increases in going from inner-valence to the shallow-core (S and Cl 2p) ionizations. Furthermore, C^+ ions are observed at all photon energies studied with the larger relative intensity (4.5%) at 200.7 eV in the Cl 2p region denoting the importance of atomization processes.

These results compare fairly well with the dissociation behavior reported for the related species CCl_4. As suggested for Cl 2p excited CCl_4,[50] dication states with two holes in the inner valence orbitals preferentially fragment via many body/multistep reactions that lead to an almost complete atomization of the products. For $CHCl_3$, it was also suggested that ultrafast fragmentation of the system following 2p excitation to a strongly antibonding (σ^*_{C-Cl}) state contributes to the large amount of Cl^+ observed in the PEPICO spectrum measured at the Cl 2p edge.[7]

These common features also determined in the present study seem to be relevant aspects for explaining the dissociation of highly chlorinated species. In connection with the stratospheric processes, the high production of chlorine ions or atoms over the whole range of photon energies used in this work can be also mentioned.

Acknowledgment. This work has been largely supported by the Brazilian Synchrotron Light Source (LNLS) under proposal D05A-TGM-6535. We thank Arnaldo Naves de Brito and his research group for fruitful discussions and generous collaboration during the several stays in Campinas and the TGM beamline staff for their assistance throughout the experiments. We acknowledge the Agencia Nacional de Promoción Científica y Tecnológica (ANPCyT), Consejo Nacional de Investigaciones Científicas y Técnicas (CONICET), and the Comisión de Investigaciones Científicas de la Provincia de Buenos Aires (CIC), República Argentina, for financial support. We also thank the Facultad de Ciencias Exactas, Universidad Nacional de La Plata, República Argentina for financial support. C.O.D.V. especially acknowledges the DAAD, which generously sponsors the DAAD Regional Program of Chemistry for the República Argentina supporting Latin American students in earning their Ph.D. in La Plata.

References and Notes

(1) Thissen, R.; Hubin-Franskin, M. J.; Furlan, M.; Piette, J. L.; Morin, P.; Nenner, I. *Chem. Phys. Lett.* **1992**, *199*, 102.

(2) Schmelz, H. C.; Reynaud, C.; Simon, M.; Nenner, I. *J. Chem. Phys.* **1994**, *101*, 3742.

(3) Miron, C.; Simon, M.; Leclercq, N.; Hansen, D. L.; Morin, P. *Phys. Rev. Lett.* **1998**, *81*, 4104.

(4) Lin, J. J.; Chen, Y.; Lee, Y. Y.; Lee, Y. T.; Yang, X. *Chem. Phys. Lett.* **2002**, *361*, 374.

(5) Sato, H. *Annu. Rep. Prog. Chem., Sect. C: Phys. Chem.* **2004**, *100*, 73.

(6) Santos, A. C. F.; Maciel, J. B.; de Souza, G. G. B. *J. Electron Spectrosc. Relat. Phenom.* **2007**, *156−158*, 236.

(7) Lago, A. F.; Santos, A. C. F.; de Souza, G. G. B. *J. Chem. Phys.* **2004**, *120*, 9547.

(8) Lago, A. F.; Santos, A. C. F.; Stolte, W. C.; Schlachter, A. S.; de Souza, G. G. B. *J. Electron Spectrosc. Relat. Phenom.* **2005**, *144−147*, 161.

(9) Lago, A. F.; Santos, A. C. F.; de Souza, G. G. B. *Int. J. Mass Spectrom.* **2007**, *262*, 187.

(10) Sundin, S.; Saethre, L. J.; Sorensen, S. L.; Ausmees, A.; Svensson, S. *J. Chem. Phys.* **1999**, *110*, 5806.

(11) Thissen, R.; Simon, M.; Hubin-Franskin, M.-J. *J. Chem. Phys.* **1994**, *101*, 7548.

(12) Erben, M. F.; Romano, R. M.; Della Védova, C. O. *J. Phys. Chem. A* **2004**, *108*, 3938.

(13) Geronés, M.; Erben, M. F.; Romano, R. M.; Della Védova, C. O. *J. Electron Spectrosc. Relat. Phenom.* **2007**, *155*, 64.

(14) Erben, M. F.; Romano, R. M.; Della Védova, C. O. *J. Phys. Chem. A* **2005**, *109*, 304.

(15) Erben, M. F.; Geronés, M.; Romano, R. M.; Della Védova, C. O. *J. Phys. Chem. A* **2007**, *111*, 8062.

(16) Geronés, M.; Erben, M. F.; Romano, R. M.; Della Védova, C. O.; Yao, L.; Ge, M. *J. Phys. Chem. A* **2008**, *112*, 2228.

(17) Erben, M. F.; Della Védova, C. O *Inorg. Chem.* **2002**, *41*, 3740.

(18) Geronés, M.; Downs, A. J.; Erben, M. F.; Ge, M.; Romano, R. M.; Yao, L.; Della Védova, C. O. *J. Phys. Chem. A* **2008**, *112*, 5947.

(19) Erben, M. F.; Geronés, M.; Romano, R. M.; Della Védova, C. O *J. Phys. Chem. A* **2006**, *110*, 875.

(20) Cortés, E.; Erben, M. F.; Geronés, M.; Romano, R. M.; Della Védova, C. O. *J. Phys. Chem. A* **2009**, *113*, 564.

(21) Rathke, B. *Ann.* **1873**, *167*, 195.

(22) Kittleson, A. R. *Science* **1952**, *115*, 84.

(23) Islam, N. B.; Kwart, H.; Khan, S. *J. Chem. Eng. Data* **1985**, *30*, 509.

(24) Kittleson, A. R. *J. Agric. Food Chem.* **1953**, *1*, 677.

(25) Sosnovsky, G. *Chem. Rev.* **1958**, *58*, 509.

(26) Senning, A. *Chem. Rev.* **1965**, *65*, 385.

(27) Della Védova, C. O.; Aymonino, P. J. *J. Raman Spectrosc.* **1986**, *17*, 485.

(28) Du, L.; Yao, L.; Zeng, X.; Ge, M.; Wang, D. *J. Phys. Chem. A* **2007**, *111*, 4944.

(29) de Fonseca, P. T.; Pacheco, J. G.; Samogin, E.; de Castro, A. R. B. *Rev. Sci. Instrum.* **1992**, *63*, 1256.

(30) Kivimaki, A.; Ruiz, J. A.; Erman, P.; Hatherly, P.; Garcia, E. M.; Rachlew, E.; Riu, J. R.; Stankiewicz, M. *J. Phys. B: At., Mol. Opt. Phys.* **2003**, 781.

(31) Frasinski, L. J.; Stankiewicz, M.; Randall, K. J.; Hatherly, P. A.; Codling, K. *J. Phys. B: At., Mol. Opt. Phys* **1986**, *19*, L819.

(32) Eland, J. H. D.; Wort, F. S.; Royds, R. N. *J. Electron Spectrosc. Relat. Phenom.* **1986**, *41*, 297.

(33) Naves de Brito, A.; Feifel, R.; Mocellin, A.; Machado, A. B.; Sundin, S.; Hjelte, I.; Sorensen, S. L.; Bjorneholm, O. *Chem. Phys. Lett.* **1999**, *309*, 377.

(34) Burmeister, F.; Coutinho, L. H.; Marinho, R. R.; Homem, M. G. P.; de Morais, M. A. A.; Mocellin, A.; Björneholm, O.; Sorensen, S. L.; de Fonseca, P. T.; Lindgren, A.; Naves de Brito, A. *J. Electron Spectrosc. Relat. Phenom.* **2008**, in press, http://dx.doi.org/10.1016/j.elspec.2006.05.007.

(35) Laskin, J.; Lifshitz, C. *J. Mass Spectrom.* **2001**, *36*, 459.

(36) Hansen, D. L.; Arrasate, M. E.; Cotter, J.; Fisher, G. R.; Hemmers, O.; Leung, K. T.; Levin, J. C.; Martin, R.; Neill, P.; Perera, R. C. C.; Sellin, I. A.; Simon, M.; Uehara, Y.; Vanderford, B.; Whitfield, S. B.; Lindle, D. W. *Phys. Rev. A* **1998**, *58*, 3757–3765.

(37) Simon, M.; LeBrun, T.; Morin, P.; Lavollée, M.; Maréchal, J. L. *Nucl. Instrum. Methods* **1991**, *B62*, 167.

(38) Pilling, S.; Lago, A. F.; Coutinho, L. H.; Castilho, R. B.; de Souza, G. G. B.; Naves de Brito, A. *Rapid Commun. Mass Spectrom.* **2007**, *21*, 3646.

(39) Santos, A. C. F.; Lucas, C. A.; de Souza, G. G. B. *J. Electron Spectrosc. Relat. Phenom.* **2001**, *114−116*, 115.

(40) Du, L.; Yao, L.; Ge, M. *Chin. J. Chem. Phys.* **2008**, *21*, 93.

(41) Nenner, I.; Beswick, J. A. Molecular Photodissociation and Photoionization. In *Handbook on Synchrotron Radiation*; Marr, G. V., Ed.; Elsevier Science Publishers: Amsterdam, 1987; Vol. 2, p 355.

(42) Hudson, E.; Shirley, D. A.; Domke, M.; Remmers, G.; Puschmann, A.; Mandel, T.; Xue, C.; Kaindl, G. *Phys. Rev. A* **1993**, *47*, 361.

(43) Svensson, S.; Naves de Brito, A.; Keane, M. P.; Correia, N.; Karlsson, L. *Phys. Rev. A* **1991**, *43*, 6441–6443.

(44) Fournier, P. G.; Comtet, G.; Fournier, J.; Svensson, S.; Karlsson, L.; Keane, M. P.; Naves de Brito, A. *Phys. Rev. A* **1989**, *40*, 163.

(45) Grant, R. P.; Harris, F. M.; Andrews, S. R.; Parry, D. E. *Int. J. Mass Spectrom. Ion Processes* **1995**, *142*, 117.

(46) Smith, D. M.; Tuckett, R. P.; Yoxall, K. R.; Codling, K.; Hatherly, P. A. *Chem. Phys. Lett.* **1993**, *216*, 493.

(47) Kinugawa, T.; Hikosaka, Y.; Hodgekins, A. M.; Eland, J. H. D. *J. Mass Spectrom.* **2002**, *37*, 854.

(48) Kime, Y. J.; Driscoll, D. C.; Dowben, P. A. *J. Chem. Soc., Faraday Trans. 2* **1987**, *83*, 403.

(49) Kischlat, W.; Morgner, H. *J. Electron Spectrosc. Relat. Phenom.* **1985**, *35*, 273.

(50) Fainelli, E.; Maracci, F.; Platania, R.; Avaldi, L. *J. Electron Spectrosc. Relat. Phenom.* **2001**, *119*, 81.

(51) Eland, J. H. D. *Mol. Phys.* **1987**, *61*, 725.

(52) Simon, M.; Lebrun, T.; Martins, R.; de Souza, G. G. B.; Nenner, I.; Lavollee, M.; Morin, P. *J. Phys. Chem.* **1993**, *97*, 5228.

(53) Eland, J. H. D. *Acc. Chem. Res.* **1989**, *22*, 381.

JP904515U